RGNZ/MGPB

Data-driven and knowledge-driven MARCOS method to Cu porphyry prospectivity modelling, a case study, Shahr-e-Babak area, southeastern Iran

Rudarsko-geološko-naftni zbornik
(The Mining-Geology-Petroleum Engineering Bulletin)
DOI: 10.17794/rgn.2026.3.3

Original scientific paper

Moslem Jahantigh[1] ✉, **Hamidreza Ramazi**[1] ✉
[1] *Faculty of Mining engineering, Amirkabir University of Technology, Hafiz Street, Tehran, Iran.*

Abstract
The present study aims to compare the performance of data-driven and knowledge-driven Multi-Criteria Decision-Making (MCDM) in producing a mineral potential model in the Shahr-e-Babak study area in south-eastern Iran. To achieve this goal, eight evidential layers, including geological, Cu signature, principal component analysis, argillaceous alteration, phyllic alteration, iron oxide alteration (Gossan), airborne geophysics layers, and linear structures, were pre-processed and produced. To produce the optimal model, first, all layers were scaled and shifted to the zero to one interval. To create the mineral potential model in the area, the Measurement Alternatives and Ranking according to Compromise Solution (MARCOS) method was introduced. For the exploration control layer weighting, two methods were used: the area prediction rate (P-A) method and the Analytic Hierarchy Process (AHP) method. Then, the results were compared with the Multi-Objective Optimization by Ratio Analysis (MOORA) method, which is a proven method in mineral potential assessment. To compare these methods, two methods – area prediction rate and the area under the curve (AUC) – were used. The findings show that the data-driven MARCOS approach provides the best performance and displays the best mineral potential model. The normalized density for the data-driven MARCOS, data-driven MOORA, knowledge-driven MARCOS, and knowledge-driven MOORA methods is equal to 3.00, 2.84, 2.7, and 2.57, respectively. The AUC for the data-driven MARCOS, data-driven MOORA, knowledge-driven MARCOS, and knowledge-driven MOORA methods is equal to 0.939, 0.938, 0.933, and 0.932, respectively.

Keywords:
Porphyry, MARCOS, MOORA, Shahr-e-Babak, Data-driven

1. Introduction

The primary step in the exploration of economic mineral resources is the identification of areas with high potential. Identifying and exploring minerals is inherently time-consuming and costly (**Feizi et al., 2021; Karbalaeiramezanali et al., 2025; Riahi et al., 2023; Tešić et al., 2023**). Therefore, it is necessary and mandatory to limit the areas to be explored. Mineral Potential Modelling (MPM) is a fundamental and key method in integrating geoscience data sets (geophysics, geochemistry, geology, remote sensing, etc.). The primary objective of MPM is to identify potential mineral areas within the study areas. The primary function of MPM is to increase the profitability of mining projects and reduce the risk related to cost and time. There are three basic steps in MPM: the first step is to identify and collect information related to the study area and the studied deposit. The second step is to weigh the exploration witness maps related to the target deposit. The third and final step is to integrate the exploration witness maps and determine the potential and mineral potential areas. Data integration is done through various operators and complex mathematical functions. This integration is done to determine target areas and potential areas of mineral potential (**Mami Khalifani et al., 2025**).

In the last decade, Geographic Information System (GIS) software has become an important tool to prioritize potential areas for minerals by integrating spatial science data. Various methods have been proposed to produce MPM based on GIS software. These methods are categorized into two categories: data-driven and knowledge-driven. In data-driven methods, known mineralization points are used to train and generate mineral models (**Tshanga et al., 2024**). Also, by relying on these points, the degree of relationship between exploration witness layers and the type of target deposit can be examined. Some data-driven methods include Support Vector Machine (SVM), Random Forest Algorithm (RF), Adaptive Neuro-Fuzzy Inference System (ANFIS), and Convolutional Neural Network (CNN). MCDM methods have been used in the past mainly in a knowledge-based manner, and expert knowledge has been used to weight the exploratory evidence layers.

* Corresponding author: Hamidreza Ramazi
e-mail address: ramazi@aut.ac.ir
Received: 11 June 2025. Accepted: 1 November 2025.
Available online: 14 May 2026

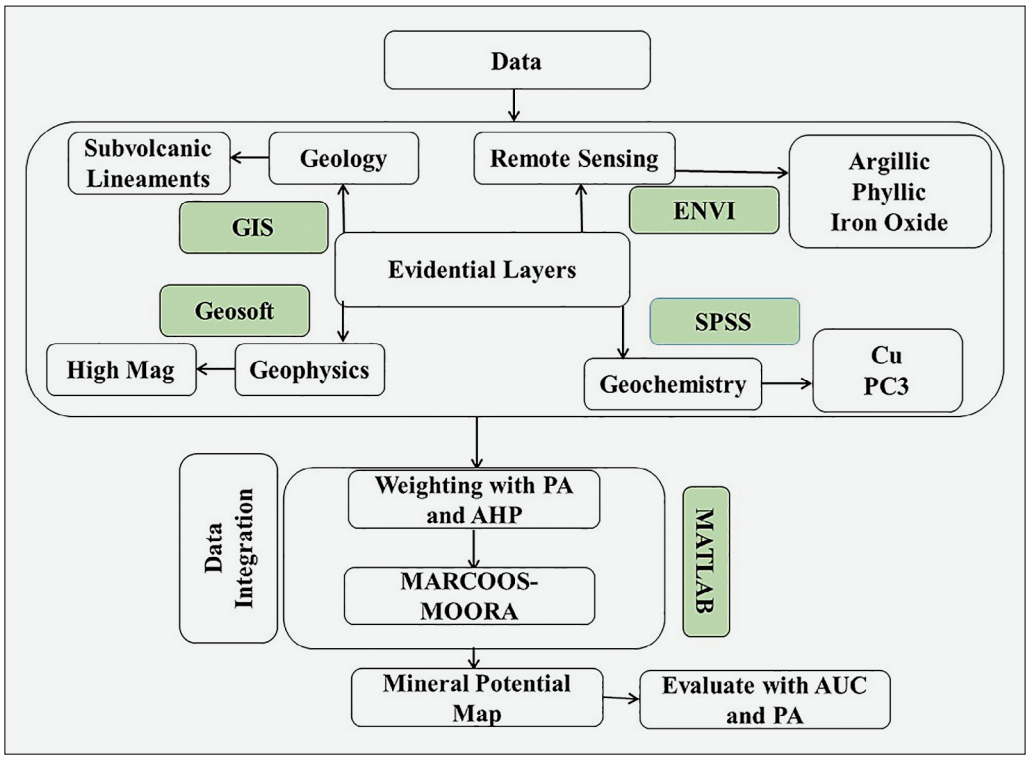

Figure 1. Flowchart of recent research on porphyry prospectivity modelling.

Knowledge-based methods are suitable for areas that have not been explored or where few mineralization points of the target deposit type have been identified. Knowledge-based methods are based on the experience of geoscientists. These methods use the knowledge of geoscientists to weigh the layers of exploratory evidence. They contain such methods of index overlay (**Bonham-Carter et al., 1989, Carranza et al., 1999, Mirzaei et al., 2014**), fuzzy logic (**An et al., 1991, Brown et al., 2000, Porwal et al., 2003, Nykänen et al., 2008, Parsa et al., 2016**), Boolean logic. (**Bonham-Carter et al. 1989**), the outranking method (**Abedi et al., 2012**), wildcat mapping (**Carranza, 2010**), Dempster-Shafer belief theory (**Moon, 1990**), and multi-criteria decision-making approaches (**Pazand et al., 2015; Yousefi & Carranza, 2015**). Over the past decade, new methods have become popular, often used in combination. In these methods, the mineralization points in the area are used to select and weight the exploration witness layers. In many studies, a combination of two or more MCDM methods has been used to make better decisions and solve the MPM problem. In fact, to successfully solve an MPM problem, it is necessary to select appropriate exploration witness layers and then generate an MPM map. From this perspective, MPM is considered an MCDM method. In fact, the application of MCDM methods in a data-driven manner enables geoscientists to reduce uncertainties for the MPM problem and eliminate inconsistencies between criteria.

In the present study, knowledge-based and data-based methods have been used to weight the exploration witness layers. Then, the obtained weights have been applied to the exploration witness layers. The weighted layers have been merged using the MOORA method, a proven approach for producing a mineral potential model. Additionally, this paper introduces the MARCOS method as a novel approach for creating a mineral potential model. The results obtained using the Marcus method have been compared with those obtained using the Mora method.

The flowchart of recent research is shown in **Figure 1.**

2. Geology and Cu Mineralization in the study area

2.1. Geology

The study area is located in the areas with the following coordinates: 55° 6.5′ to 55° 20′ east longitude and 30° 20′ to 30° 27′ north latitude (see **Figure 2a** and **b**). In this area, several Mio-Pliocene dacite-andesite volcanic masses have erupted into the rocks of the Urmia-Dokhtar magmatic belt in the form of domes or small volcanic cones that are located in the south and northeast of the Masahim Volcano. The age of these masses is reported to be Mio-Pliocene based on the Shahr-e-Babak geological map (**Safari et al., 2018**). The volcanic rocks related to the Eocene are older, and the dacite-andesite masses have intruded them and are younger, containing older fragments. The high altitude compared to the adjacent Eocene volcanic rocks and the light colour of the dacite rocks distinguish these masses from other rocks in

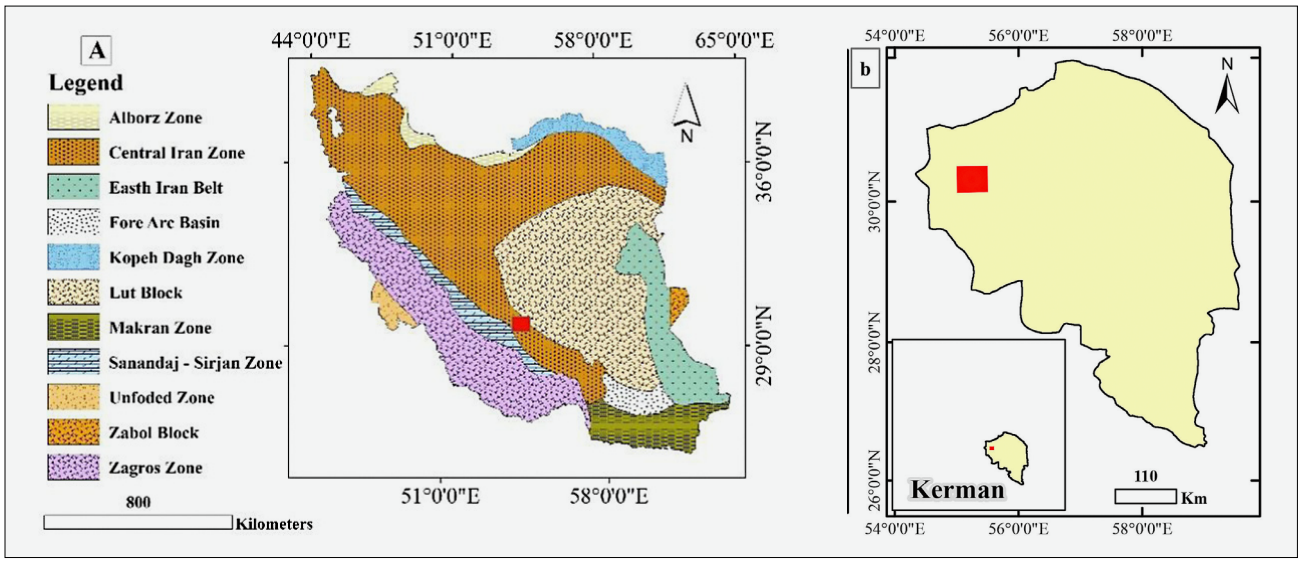

Figure 2. Location of Shahr-e-Babak in Iran structural zones map. b Location of Shahr-e-Babak in Kerman Province.

the region. In the study area, the andesitic units of the region have been investigated and studied. The andesites of the region are seen in the desert in the form of lava flows and dykes (see **Figure 3**). Andesitic dykes are younger than the lavas (**Jahantigh & Ramazi, 2024; Jahantigh & Ramazi, 2025**). In terms of petrological characteristics, most of the andesites have a porphyry texture in which plagioclase, amphibole, and pyroxene crystals are noticeable.

2.2. Cu mineralization (Cu indices) in the study area

Several porphyry copper deposits have been identified in the Shahr-e-Babak area. Some of these deposits, such as the Miduk, Sara, Dareh-Hezar, and Abdar deposits, are involved in the world-class porphyry copper deposits. Exploration drilling operations have been carried out in some active porphyry mines of the study area, including Miduk, Sara Dareh Hezar, and Abadar, and the reserves of these mines have been estimated, such as 0.224 Mt and a grade of 2.147% in Miduk and 1.825 Mt and a grade of 1.06% in Abadar (**Taghipour et al., 2008**). The porphyry copper indices and mines of the study area are presented in **Table 1** and **Figure 4.**

3. Conceptual model for Porphyry Cu-Au Deposits

Porphyry copper deposits in Iran are consistent with Tertiary volcano-plutonic belts and are located within the Tethys belt (**Waterman & Hamilton, 1975**). In Iran, calk-alkaline volcano-plutonic rocks in the Urmia-Dokhtar magmatic arc have a high potential for exploration of Cu±Mo±Au deposits, so many of the most important porphyry copper deposits in Iran are located from the northwest to the southeast of Urmia-Dokhtar (**Shahabpour, 1999**). In terms of tectonic setting, a significant part of porphyry copper deposits are formed at the margins of convergent plates (active continental margins and arc islands). Porphyry copper systems are prominently distributed in subduction zones associated with continents and island arcs. Subduction is a characteristic feature of these regions; however, other metallogenic factors also control the formation of these deposits (**Sillitoe, 1994**). It has been shown that the formation of porphyry copper deposits is not only controlled by hydrothermal and magmatic processes, but also by regional tectonics at the time of the formation of these deposits (**Sillitoe, 1994; Richards et al., 2001**).

Exploration of porphyry deposits is mainly possible with the help of geological, geochemical, geophysical, and remote sensing studies, and their detailed study will significantly contribute to the exploration of porphyry copper deposits.

Geochemical studies, particularly the geochemistry of stream sediments, play a significant role in identifying hidden reserves. It is primarily a good guide in determining the location of porphyry systems. Additionally, multivariate methods, such as principal component analysis, can be employed to more effectively identify the impact of porphyry systems (**Nathan et al., 2021**).

Geophysical methods help to explore and characterize porphyry copper deposits at all scales. At the regional scale, the airborne magnetometer method provides insights into the large-scale crustal structure and magmatic setting of mineralizing zones. Fault zones, sedimentary basins, and masses can be mapped and characterized using airborne magnetic data.

Remote sensing is another important tool for regional-scale exploration of porphyry copper deposits. Argillaceous, phyllic, and iron oxide alteration have distinct spectral absorption features that can be mapped using multispectral and hyperspectral remote sensing data (**Mars, 2006**).

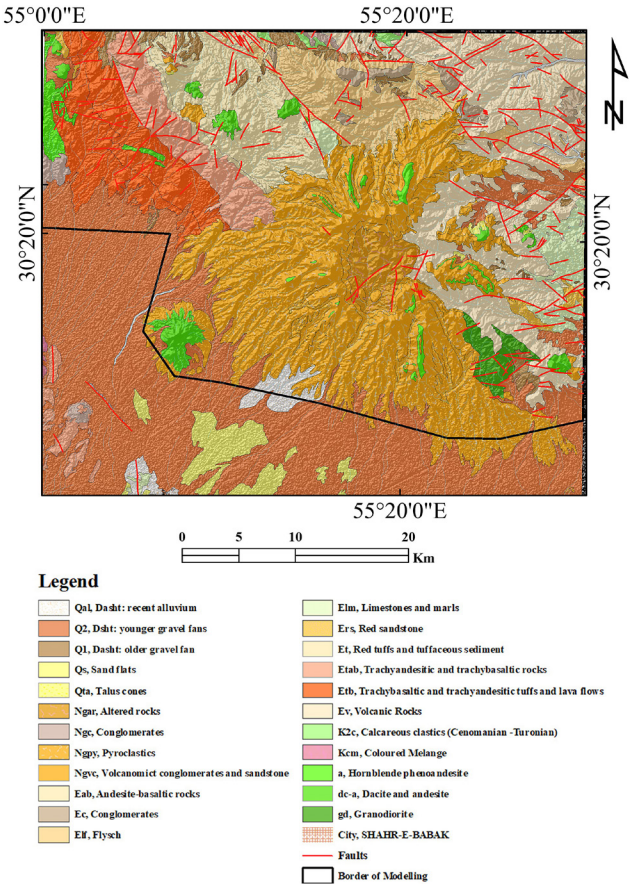

Figure 3. Geology map of the Shahr-e-Babak study area.

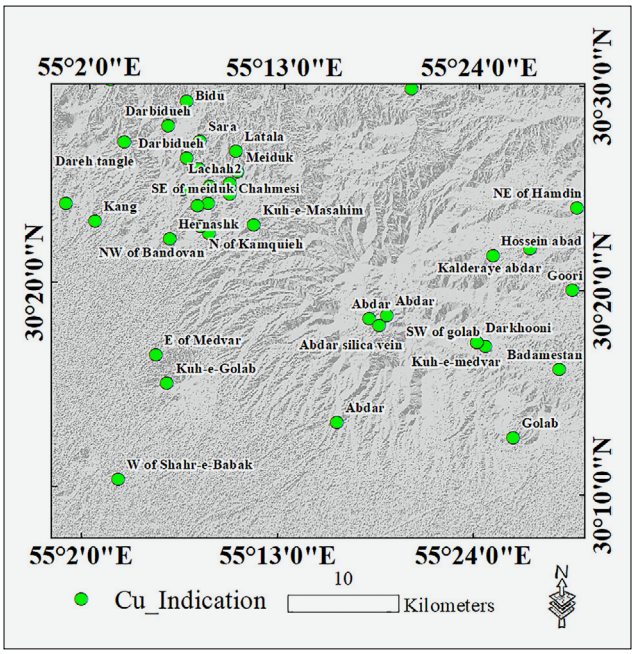

Figure 4. Location of Cu indication on digital elevation model of the Shahr-e-Babak study area.

Fractures and vein systems, as well as shear, are inevitable consequences of porphyry magmatism. Trans-compressive tectonics are characterized by strike-slip faults with significant reverse motion in highly compressive environments. Stress relief is accompanied by the

Table 1. Important Cu indication in the Shahr-e-Babak study area

Name	X	Y	Name	X	Y
Bidu	55.125	30.483	South of Miduk	55.137	30.398
Kuh-e-Masahim	55.190	30.383	Hossein abad	55.415	30.361
Miduk	55.174	30.426	SW of golab	55.409	30.287
Sara	55.138	30.451	Darkhooni	55.401	30.290
E of Medvar	55.100	30.276	Golab	55.436	30.213
Kahatookara	55.013	30.398	Kuh-e-medvar	55.401	30.290
W of Shahr-e-Babak	55.067	30.174	NE of Hamdin	55.493	30.401
Kang	55.041	30.384	Goori	55.490	30.334
Dareh tangle	55.067	30.449	Badamestan	55.479	30.269
S of Miduk silica vein	55.167	30.413	Abdar	55.300	30.308
Kuh-e-Golab	55.111	30.253	Chahmesi	55.167	30.408
Hernashk	55.111	30.371	Abdar	55.271	30.223
Darbidueh	55.126	30.437	Lachah2	55.167	30.417
Darbidueh	55.108	30.463	Kalderaye abdar	55.450	30.367
E of Miduk station	55.123	30.411	NW of Miduk	55.138	30.428
W of Miduk station	55.148	30.414	Godkalgovari	55.053	30.500
NW of Bandovan	55.148	30.376	Reshkan	55.336	30.496
N of Kamquieh	55.140	30.381	Abdar silica vein	55.309	30.303
SE of Miduk	55.147	30.400	Abdar	55.316	30.311
			Latala	55.172	30.443

emplacement of mineralized porphyry intrusions (**Richards et al., 2001**). The injection of these intrusive masses is accompanied by the injection of mechanical energy and steam from the magma, which leads to fractures that are characteristic of porphyry deposits.

Porphyry copper deposits are mainly formed in the upper crust of the Earth (depth less than 5 to 10 km), on the margins of active convergent, and usually in high-altitude areas or areas that are subject to high rates of uplift.

Building a conceptual model for regional exploration is a key point in quantitative mineral resource prediction. A conceptual model refers to a written representation of a mineral resource model that is used in various methods of mineral potential modelling, and, along with various features of the deposit controller, the effects and integration of data (including assumptions and genesis), deposit models, regional exploration models, and local exploration models are used as a guide for predicting mineral resources. In this study, a conceptual model of porphyry copper has been used for mineral resource exploration.

4. Methods

4.1. MCDM method for mineral potential modelling

4.1.1. MARCOS method

The MARCOS method consists of 7 steps, which were first introduced by **Stević et al. (2020)**. The steps of the Markov method are as follows:

Step 1: Create an initial decision matrix. This decision matrix includes n criteria and m alternatives.

Step 2: Create an initial matrix based on an extended initial matrix. In this step, for creating a decision matrix, the ideal (AI) and anti-ideal (AAI) solution will be defined.

The anti-ideal solution (AAI) is the worst alternative, while the ideal solution (AI) is an alternative with the best characteristic. Depending on the nature of the criteria, AAI and AI are defined by applying **Equations 1** and **2**:

$$AAI = minx_{ij} \quad if\ j\varepsilon\ B\ and \quad maxx_{ij} \quad if \quad j\varepsilon\ C \quad (1)$$

$$AI = maxx_{ij} \quad if\ j\varepsilon\ B\ and \quad minx_{ij} \quad if \quad j\varepsilon C \quad (2)$$

Where B is the utility group of criteria, while C represents a group of cost criteria

Step 3: in the third step the extended initial matrix should be normalized.

Step 4: in this step, the weight matrix should be determined.

Step 5: in this step, the utility degree of the alternative k_i should be calculated. By multiplying the following equation, the utility degree of an alternative related to ideal and anti-ideal is calculated. The s_{aai} and s_{ai} are the elements of the decision matrix.

$$\boldsymbol{k_i^-} = \frac{\boldsymbol{s_i}}{\boldsymbol{s_{aai}}} \quad (3)$$

$$\boldsymbol{k_i^+} = \frac{\boldsymbol{s_i}}{\boldsymbol{s_{ai}}} \quad (4)$$

$\boldsymbol{s_i}$ is the summation of all elements of weighted matrix V, as shown in the following equation:

$$\boldsymbol{s_i} = \sum_{i=1}^{n} \boldsymbol{v_{ij}} \quad (5)$$

Step 6: in this step determination of the utility function of alternative $\boldsymbol{f(k_i)}$ should be calculated. The utility function is the compromise of the observed alternative about the ideal and anti-ideal solution. The utility function of alternatives can be calculated from the following equation:

$$f(k_i) = \frac{k_i^+ + k_i^-}{1 + \frac{1 - f(k_i^+)}{f(k_i^+)} + \frac{1 - f(k_i^-)}{f(k_i^-)}} \quad (6)$$

Where $\boldsymbol{f(k_i^-)}$ is the beneficial function related to the anti-ideal solution and $\boldsymbol{f(k_i^+)}$ is the beneficial function related to the ideal solution.

Beneficial functions related to the ideal and anti-ideal solutions can be calculated from the following equation:

$$\boldsymbol{f(k_i^-)} = \frac{\boldsymbol{k_i^+}}{\boldsymbol{k_i^+ + k_i^-}} \quad (7)$$

$$\boldsymbol{f(k_i^+)} = \frac{\boldsymbol{k_i^-}}{\boldsymbol{k_i^+ + k_i^-}} \quad (8)$$

Step 7: in the final step the ranking of alternatives is distinguished. Ranking of alternatives is based on beneficial function.

After calculating the seven steps that were mentioned the MARCOS model was generated.

4.1.2. MOORA

The MOORA method is widely regarded as valuable for improving the best alternatives and determining the most viable substitute among a set of options in multi-criteria decision-making (**Brauers & Zavadskas, 2006; Jahantigh & Ramazi, 2024**).

To achieve this objective, the subsequent measures need to be implemented:

- Step 1: The process includes developing and producing a decision matrix
- Step 2: The process includes normalizing the decision matrix.
- Step 3: Determination of the vector of weights for criteria with the AHP method.
- Step 3: The process involves enhancing various qualities by incorporating standardized achieve-

ment when maximizing (positive qualities) and subtracting when minimizing (negative qualities).

- Step 4: To predict a specific event accurately, it is important to consider that certain attributes hold more significance.

4.2. Prediction-Area (P-A) plot (Data-driven method)

Using the P-A model and determining the prediction rate according to the intersection point can determine the order and relative importance of the evidence maps as criteria related to the type of mineralization under investigation. Furthermore, using values on both the right and left axes of this graph can be used to weight the evidence layers as a data-driven method. Since the main objective of the present study is to obtain a potential map for identifying porphyry copper mineralization, obtaining quantitative weights for each layer is required. We can obtain a normalized density quantity by calculating the ratio of the prediction rate to the corresponding occupied area. The following equations explain the use of the P-A model (**Yousefi & Carranza, 2015**):

$$N_d = \frac{P_r}{Q_a} \tag{9}$$

The N_d normalized density, P_r is the predicted rate and Q_a is the area occupied by mineralization, which is extracted from the intersection point of the P-A model. Normal density is used to calculate the weight of each map according to the following formula:

$$W_E = \ln N_d \tag{10}$$

W_E is the final weight of each exploratory evidential layer calculated using the P-A model and the intersection point of its graph.

Data-driven models are based on the spatial relationship between the exploration witness layers and the mineralization points. The factors affecting mineralization are very complex and may be outside the view and knowledge of geoscientists, causing errors in the production of the mineral potential model. Data-driven methods address this deficiency and improve the mineral potential model produced.

4.3. Analytic Hierarchy Process (AHP) (knowledge driven method)

Saaty (1977) first introduced the analytical hierarchy process (AHP), widely recognized as one of the most popular MCDM techniques. Among the advantages of this method are: measuring the consistency of decision-makers' judgments, creating pairwise comparisons in choosing the optimal solution and option, being able to consider criteria and sub-criteria in evaluating options, and creating the ability to achieve the best option through pairwise comparisons. The Analytic Hierarchy Process is a method that aids in decision-making. It emphasizes the importance of a decision-maker's intuitive judgments as well as the consistency of comparing alternative options in the decision-making process. Since a decision-maker bases his judgments on knowledge and experience, and therefore makes decisions based on them, the AHP approach is consistent with the behaviour of a decision-maker. The strength of this approach is that it systematically organizes tangible and intangible factors and provides a structured but relatively simple solution to decision-making problems.

Furthermore, by breaking down a significant logical problem and then descending in gradual steps to smaller and smaller ones, one can connect the small to the significant through simple pairwise comparison judgments. Rosaria and **Camanho (2015)** believe that AHP is a measurement tool through pairwise comparisons. This method relies on expert judgments to derive priority scales. The hierarchical decision tree of Shahr-e-Babak is shown in **Figure 5**, where the main tree creations are considered, including geochemistry signature, airborne magnetic anomaly, geology, and remote sensing. These sub-criteria consist of Cu, principal component analysis (PC3), reduction to pole (RTP), intrusive rocks, faults, argillaceous alteration, phyllic alteration, and iron oxide alteration. These criteria were used to make ready evidential layers related to Cu porphyry mineralization.

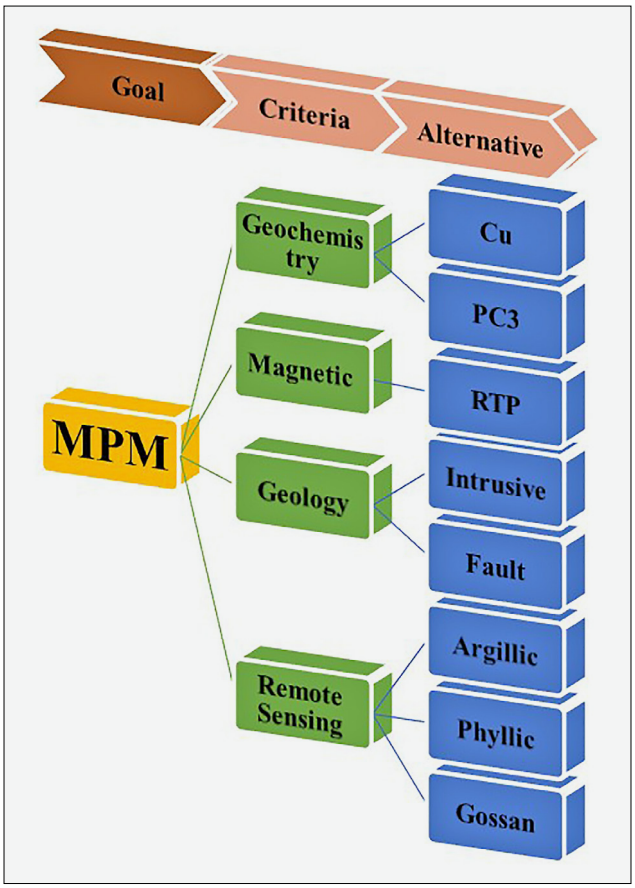

Figure 5. Hierarchy is applied for prospective modelling and weighting exploratory evidential layers

4.4. Preparing exploratory evidential layers

In modelling the mineral potential for a type of prospecting deposit, all the characteristics of the mineral type being explored are first identified and collected. At this stage, a regional conceptual model can be derived based on general studies of mineral-type reserves that exist around the world, because a good conceptual model is the best tool for identifying exploration criteria and extracting predictive patterns for the mineral of interest. To model the mineral potential of a given type of prospecting deposit in a specific region, the exploration dataset used is based on the conceptual model of that type of deposit. Then, based on the data, witness maps are generated and weighted, and finally combined to identify target areas.

To build a conceptual regional model of porphyry copper deposits in the Shahr-e-Babak, geological, geochemical, and remote sensing exploration criteria were used. Five exploration witness maps (layers), including host rock, fault density, geochemical trace, iron oxide alteration, and argillaceous, phyllic, and propylitic alteration, were generated to search for copper mineralization in the region using the continuous fuzzy method. Since these values are derived from different spatial data sets, their minimum and maximum values differ, and their spatial extents are also distinct. In this study, the values of different exploratory evidence datasets are transformed into a similar space by using the following logistic function as a nonlinear transformation (**Yousefi et al., 2021**):

$$F_E = \frac{1}{1 + e^{-s(x-i)}} \tag{11}$$

Where x is the actual value of the exploratory evidential layers and F_E is the value of the evidential layers after the logistical transformation. The s and i are the slope and inflection points of this transformation. The exploratory evidential layers are shown in **Figure 5** and the fuzzy exploratory evidential layers are shown in **Figure 7**.

Porphyry copper deposits in the Urmia-Dokhtar belt are genetically and spatially related to subvolcanic units. This relationship is because the margins of the subvolcanic units are fractured and crushed, which allows for the circulation and movement of hydrothermal fluids and, consequently, heat exchange. For this reason, the probability of porphyry copper deposits forming in areas close to and adjacent to the subvolcanic units is higher.

To produce exploratory evidential layers of the subvolcanic units in the study area, the Euclidean distance of the subvolcanic units was utilized (see **Figure 6a**). Then, to create exploratory evidential layers, **Equation 9** was employed to transform the evidential layer into the logistic space (weight space) (**Figure 7a**).

Structural studies show the important role of rock permeability in the formation of mineral deposits. In this regard, the presence of structural faulting is also generally considered an important criterion for the presence of some deposits. Faults facilitate the passage of magma and the circulation of hydrothermal fluids, and it is generally accepted that faults and fractured areas act as the primary channels for the passage of hydrothermal fluids. Faults and fractures play a role in the formation of many mineral deposits. Therefore, the presence of such geological features indicates an increase in the structural permeability of rocks in the subsurface. Therefore, areas with high fault density and fractures can transport and circulate mineralized solutions. In this paper, fault density has been used as a structural control layer for the formation of porphyry copper deposits in the study area. To produce the fault density map, the total length of the faults in each pixel of the study area, i.e. the fault density, was calculated (see **Figure 6b**). Then, since the fault density values do not have a specific range and are outside the logistic space, **Equation 9** was applied to the fault density dataset (see **Figure 7b**).

In geology and mineral exploration, airborne geophysical data are used as one of the most important sources of information to study geological features and subsurface structures, such as faults, intrusive masses, and hidden plutonic masses. The use of airborne magnetic data in obtaining magnetic information layers, structures, and edges is considered a guide for porphyry copper mineralization (**Holden et al., 2008**). The airborne magnetic data acquired by the Atomic Energy Organization of Iran (AEOI) during 1977 and 1978 were used to prepare the total magnetic intensity map of the study area. These data were obtained with a flight line spacing of about 1000 m and an altitude of about 120 m. The International Geomagnetic Reference Field (IGRF) filter was used to remove regional anomalies from the aeromagnetic map. Then, the RTP filter was performed on the total magnetic intensity map, and the anomalies were extracted from the resulting map. The fractal method was used to extract high magnetic anomalies. Then the Euclidean distance was calculated for high magnetic anomalies (see **Figure 6c**). Also, lineament structures were extracted with the tilt angle method (**Salem et al., 2007**). Magnetic lineaments were combined with geological faults, and the density map resulting from this combination was calculated. The Euclidean distance of high magnetic anomalies was transformed to the logistic space with **Equation 9** (see **Figure 7c**).

Geochemical surveys can be used at various stages of mineral resource exploration, from regional to local. The basis of geochemical exploration is the search and detection of areas where the concentration of one or more specific elements is higher than usual. In other words, with the help of geochemical exploration, areas with such anomalies are identified. The main problem in identifying anomalies in geochemical surveys of mineral exploration is the determination and inference of multi-element traces indicative of the mineralization sought. In

Table 2. Principal component analysis for multi-element geochemical data, where component 3 corresponds to Cu mineralization.

	Component		
	1	2	3
Ni	.883	-.047	.136
Ba	-.016	.818	-.056
Pb	.153	.468	.695
B	.714	-.080	.258
Co	.842	-.065	-.080
Sb	-.110	.685	.098
Cr	.615	.557	.157
Cu	.521	.295	.515
Zn	.059	-.150	.808

Table 3: Total Variance Explained

Component	Total % of Variance	Cumulative
1	27.061	27.061
2	20.258	47.319
3	17.837	65.156

this regard, principal component analysis, as one of the multivariate analysis methods, has been widely used to interpret geochemical data of stream sediments. Principal component analysis can reveal multi-element compositions from the data set that can be used as geochemical traces indicative of the mineralization type sought. Cu geochemical signature (stream sediment) has been used as an exploratory evidential layer to create a porphyry prospectivity model (see **Figure 7d**).

Also, Principal Component Analysis (PCA) method has been used for multivariate analysis and dimensionality reduction of geochemical data.. **Table 2** shows the PCA of stream sediment geochemistry data for the study area. PC3, which shows higher values of Cu, Pb, and Zn, was determined to be associated with porphyry mineralization. A geochemical map with PCA scores (PC3) was also created as another control layer. The multivariate geochemical map (PC3) is shown in **Figure 6e**. **Table 3** shows the PCs variances and Total variances from the principal component analysis of the geochemical data.

Geochemical signature layers, including the Cu signature map and geochemical map with PCA scores (PC3), were transformed to the logistic space with **Equation 9** (see **Figure 6d** and **Figure 7e**).

One of the key ideas of remote sensing techniques in exploration geology is to display rocks, minerals, and structures associated with a specific mineral type, for which several logical reasons have been presented. Therefore, given that minerals do not always emerge at the Earth's surface and due to the slight expansion of the mineralization area, remote sensing can be helpful in most cases in the search for and exploration of mineral deposits, as well as in reducing the study area. Identification and detection of alterations by remote sensing are also efficient tools in the exploration of mineral resources, and their application in deposits with broad and prominent halos has been efficient. One of the important characteristics of hydrothermal deposits is the formation of alteration halos. Iron oxide (gossan) is evidence that reinforces the possibility of the presence of porphyry copper deposits, which may extend several kilometers from the center of mineralization.

A band ratio of 3:1 was applied to detect the iron oxide alteration zone in the study area. Band ratios 7/6 and (5+7)/6 were applied for extracting argillaceous and phyllic alteration zones, respectively. The Euclidean distance maps from argillaceous, phyllic, and iron oxide alteration were created (see **Figure 6f, 6g, 6h**). The Euclidean distance maps of alteration exploratory evidential layers have been transformed to the logistic space with **Equation 9** (see **Figure 7f, Figure 7g,** and **Figure 7h**).

5. Results and Discussion

One of the basic steps in regional exploration and mineral potential assessment is to identify the exploratory evidential layers to limit the exploration area and determine the regional anomaly. Next, the effective weight of each layer is determined, and then these weights are applied to the relevant layers. Selecting appropriate weights is done in two ways. In the first method, which is the knowledge-based method, the weights of the layers are determined based on expert opinion. The second method, which is the data-driven method, selects weights based on the mineralization points in the area. In this way, the relationship between exploration layers and mineralization points is determined based on data-driven methods. Finally, the weights obtained from these methods are applied to the relevant exploratory evidential layers. In this article, the AHP, MOORA, and MARCOS methods have been used to determine mineral potential using a knowledge-based method. The relevant weights have been determined based on the AHP method. Accordingly, the pairwise comparison is shown in **Table 4**, and the weights assigned to the exploratory control layers using the AHP method are shown in **Table 5**. According to **Table 5**, the most effective layers are the univariate geochemical layer, the multivariate geochemical layer, and the subvolcanic units. The weight of all these layers is 0.211. The following effective layers are phyllic, argillaceous, and iron oxide alterations. The weights of these layers are 0.128, 0.078, and 0.078, respectively. Argillaceous and iron oxide alteration have the same weights.

The fault and geophysical layers are the least influential layers with weights of 0.049 and 0.033.

In the data-driven method, the mineralization points in the area are used to obtain the weight of the layers. Thus, by drawing a curve, the relationship between the evidential layers and the mineralization points is expressed quantitatively, and this value is considered as the

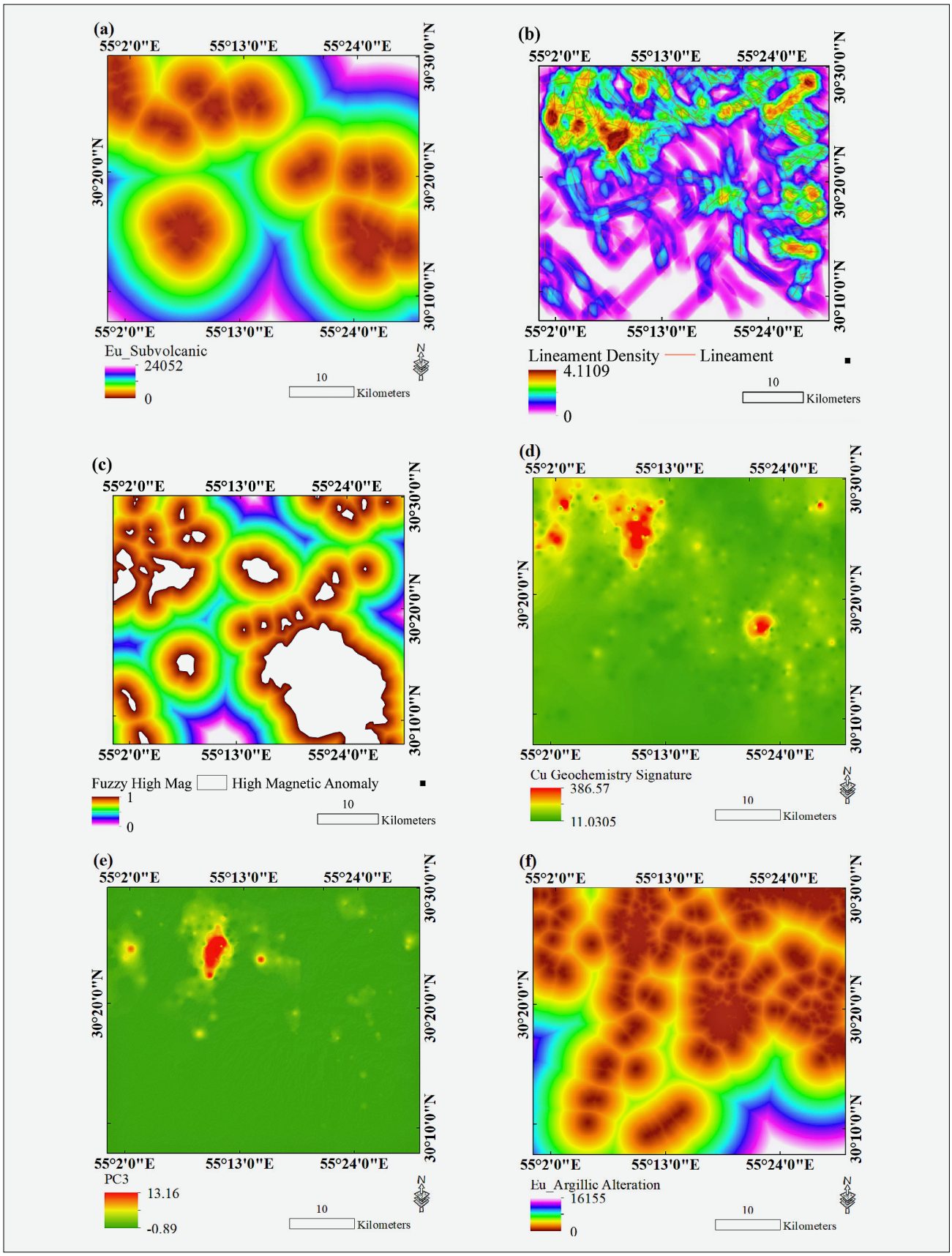

Figure 6. Evidential layer input for MPM model: (a) Euclidean distance from subvolcanic units (b) Lineament density (c) Euclidean distance from aeromagnetic anomalies (d) Cu signature (e) Multivariate geochemistry signature (PC_3) (f) Euclidean distance from argillic alteration (g) Euclidean distance from iron oxide alteration (h) Euclidean distance from phyllic alteration.

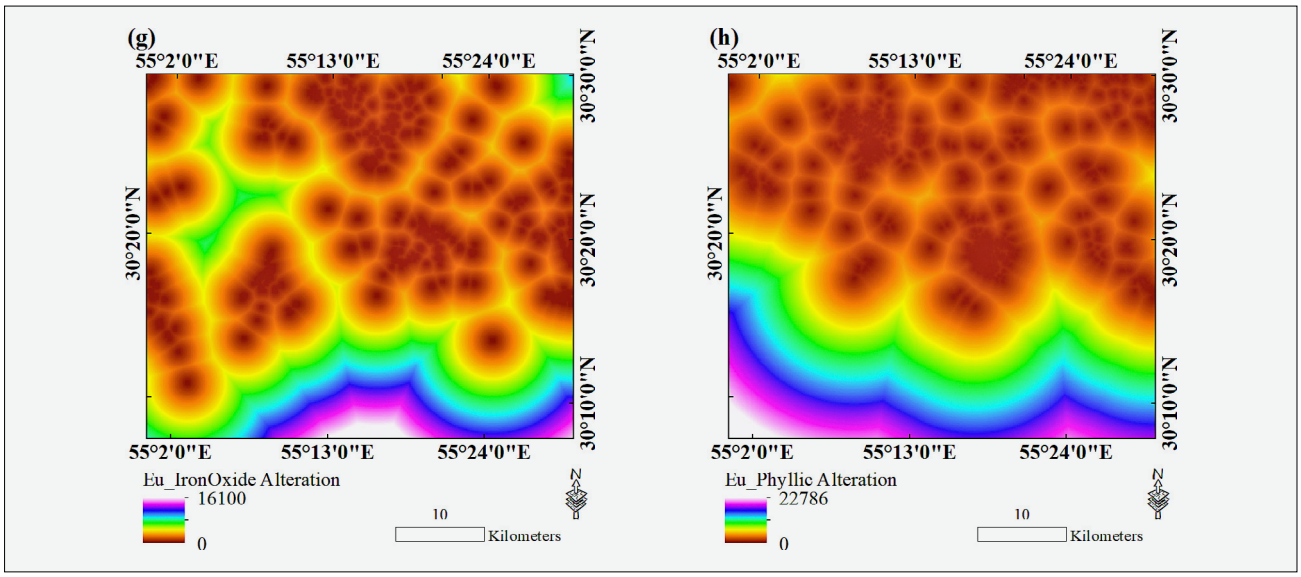

Figure 6. Continued

Table 4. Pairwise comparison matrix for exploratory control layers using the AHP method

Cu	PC3	Lithology	Phyllic	Iron Oxide	Argillic	Fault	Geophysics
1	1	1	2	3	3	4	5
1	1	1	2	3	3	4	5
1	1	1	2	3	3	4	5
0.5	0.5	0.5	1	2	2	3	4
0.33	0.33	0.33	0.5	1	1	2	3
0.33	0.33	0.33	0.5	1	1	2	3
0.25	0.25	0.25	0.33	0.5	0.5	1	2
0.2	0.2	0.2	0.25	0.33	0.33	0.5	1

Table 5. Weights calculated for exploratory evidential layers using the AHP method

Criteria	Cu	PC3	Lithology	Phyllic	Iron Oxide	Argillic	Fault	Geophysics	Weights
Cu	0.217	0.217	0.217	0.233	0.217	0.217	0.195	0.179	0.211
PC3	0.217	0.217	0.217	0.233	0.217	0.217	0.195	0.179	0.211
Intrusive	0.217	0.217	0.217	0.233	0.217	0.217	0.195	0.179	0.211
Phyllic	0.108	0.108	0.108	0.117	0.145	0.145	0.146	0.143	0.128
Iron Oxide	0.072	0.072	0.072	0.058	0.072	0.072	0.098	0.107	0.078
Argillic	0.072	0.072	0.072	0.058	0.072	0.072	0.098	0.107	0.078
Fault	0.054	0.054	0.054	0.038	0.036	0.036	0.049	0.071	0.049
Geophysics	0.043	0.043	0.043	0.029	0.024	0.024	0.024	0.036	0.033

effective weight of the evidential layer. The P-A plot method was used to draw a curve and quantify the relationship between the exploratory evidential layers and mineralization points. Based on this, the P-A plot has been drawn for eight layers of exploratory evidence (see **Figure 8**), and the normalized density (Nd) was presented for the evidential layers in **Table 6**. According to the P-A plot method, the most effective layers are the subvolcanic unit, the univariate geochemical layer, the phyllic alteration layer, the faults, and the PC3 layer, respectively. The weights of these layers are 0.84, 0.75, 0.7, 0.53, and 0.44. The least influential layers are the argillaceous alteration, iron oxide alteration, and the aeromagnetic layer. The weights of these layers are calculated to be 0.4, 0.35, and 0.23, respectively.

According to **Figure 1**, mineral potential modelling using the two methods, FAHP MOORA and FAHP MARCOS, includes four steps: (1) Selection of criteria, (2) Fuzzification of exploratory evidential layers, (3) assigning weights obtained from the AHP method on exploratory evidential layers, and (4) Use of the MOORA and MARCOS methods to combine layers and generate

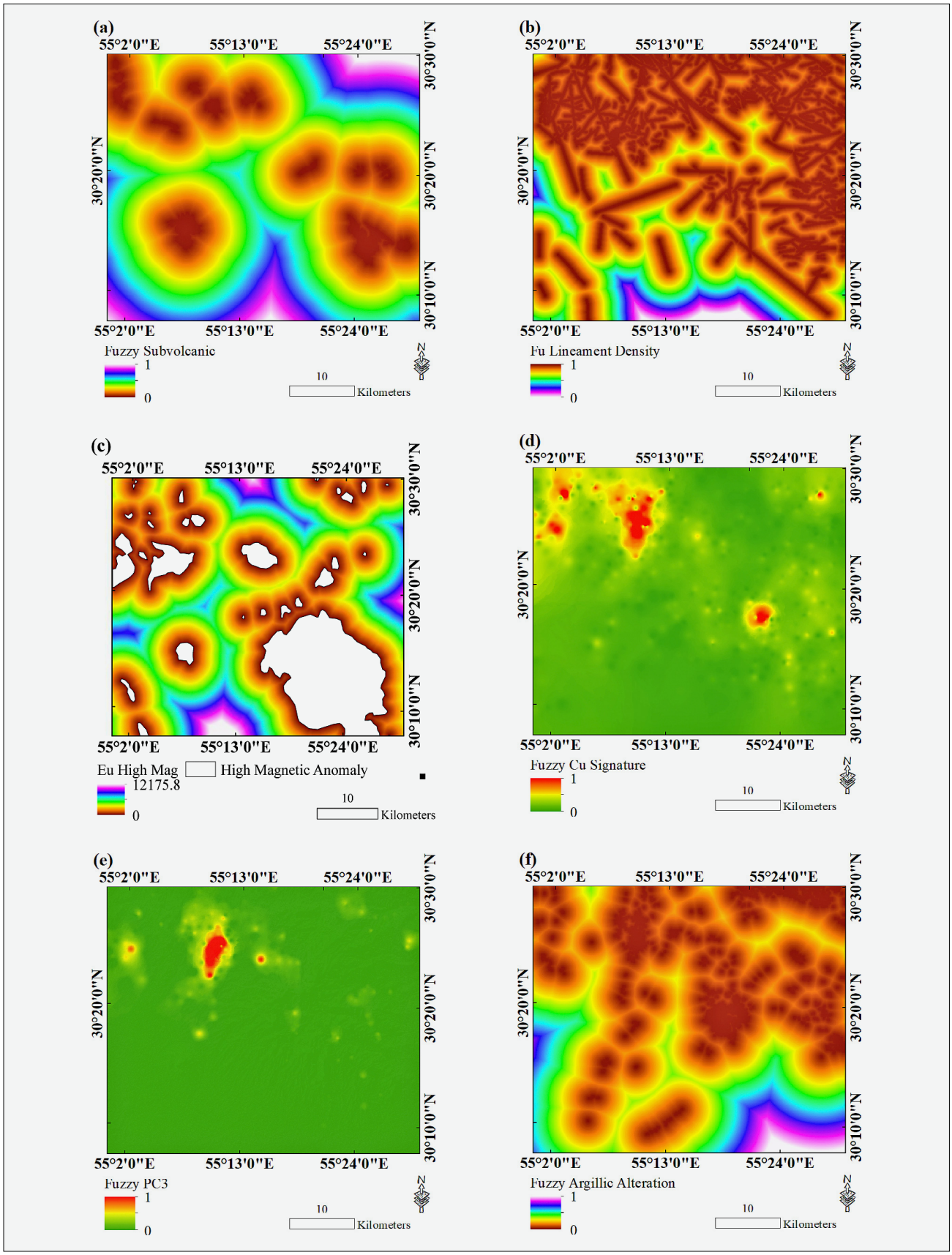

Figure 7. Fuzzified of evidential layer input for MPM model: (a) Euclidean distance of subvolcanic units (b) Lineament density (c) Euclidean distance of aeromagnetic anomalies (d) Cu signature (e) Multivariate geochemistry signature (f) Euclidean distance from argillic alteration (g) Euclidean distance from iron oxide alteration (h) Euclidean distance from phyllic alteration.

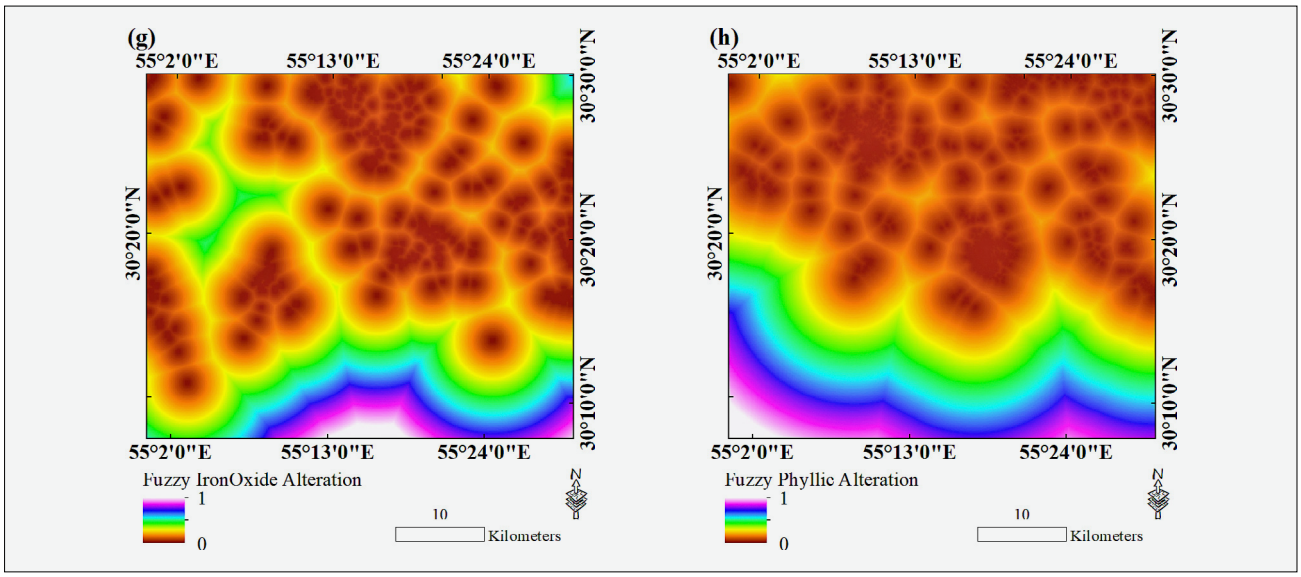

Figure 7. Continued

a mineral potential model. For the aforementioned functions, after selecting the layers, fuzzification, and assigning the weights obtained using the AHP method (see **Table 2**), a decision matrix with eight layers of exploratory evidence and 196,320 pixels is constructed. MATLAB software was used to write the code for the MOORA and MARCOS methods, and four porphyry copper mineral potential models were generated (see **Figure 9**).

In this study, two mineral potential models were generated using the MOORA and MARCOS methods. To generate the mineral potential model using data-driven methods, the weight of the exploratory evidential layers is first calculated using the porphyry copper mineralization indices. For this purpose, the P-A diagram was first drawn for eight exploratory evidential layers, using the Nd weights initially. Then, the normalized weights were calculated based on the normalized density. A decision matrix was formed for the above calculated weights. The columns of this matrix are the exploratory evidential layers derived from geological, geochemical, remote sensing, and airborne geophysical data. The rows of this matrix represent the pixels that comprise the raster maps. Finally, programming in the MATLAB environment was used to generate a porphyry copper mineral potential model using the above matrix and based on the data-driven methods of MOORA and MARCOS (see **Figure 9**).

The data-driven P-A plot method was used to evaluate and compare models produced by data-driven and knowledge-driven methods. For this purpose, 37 copper mineralization points in the area have been used. Jenks' method was used to discretize mineral potential maps. With the application of this method, the exploratory evidential layers were divided into ten parts. Based on this, the P-A plot diagrams for mineral potential models were drawn. Prediction-Area plots for the four mineral potential models are shown in **Figure 10**. In these plots, the intersection points of the prediction-area plots are specified. The intersection points for the knowledge-based MOORA, data-based MOORA, knowledge-based MARCOS, and data-based MARCOS models are 72%, 74%, 73%, and 75%, respectively. Accordingly, the normalized density values for the aforementioned models are 2.57, 2.84, 2.7, and 3, respectively. Also, the objective weights of these models are 0.94, 1.04, 0.99, and 1.09, respectively (see **Table 7**). Accordingly, the high-potential areas identified in the four models can be applied in future exploration programs, given that they have a normalized density of approximately one or greater than one.

The main characteristic curve was used to evaluate the performance of the four models. The curve obtained from the four methods shows the high accuracy of the MARCOS and MOORA methods in modelling the potential of porphyry copper in the study area. The areas under the curves of the four models, including AHP-MOORA, data-driven MOORA, AHP MARCOS, and data-driven MARCOS, are 0.932, 0.938, 0.933, and 0.939, respectively (see **Figure 11**). These values show the high accuracy of these four methods in modelling. Given that the area under the curve in the Data-Driven MARCOS method is higher than the other three methods, it indicates that the Data-Driven method has produced the potential of porphyry copper in the study area with more accuracy.

As explained in the previous section, the mineral potential model was generated using four methods: MOORA knowledge-based, MOORA data-based, MARCOS knowledge-based, and MARCOS data-based. In knowledge-based modelling methods, the AHP method was implemented to weight the layers. The pairwise comparison matrix and the calculated weights are shown in **Tables 1** and **2**, respectively. In the AHP method, the highest weights are attributed to the univariate and mul-

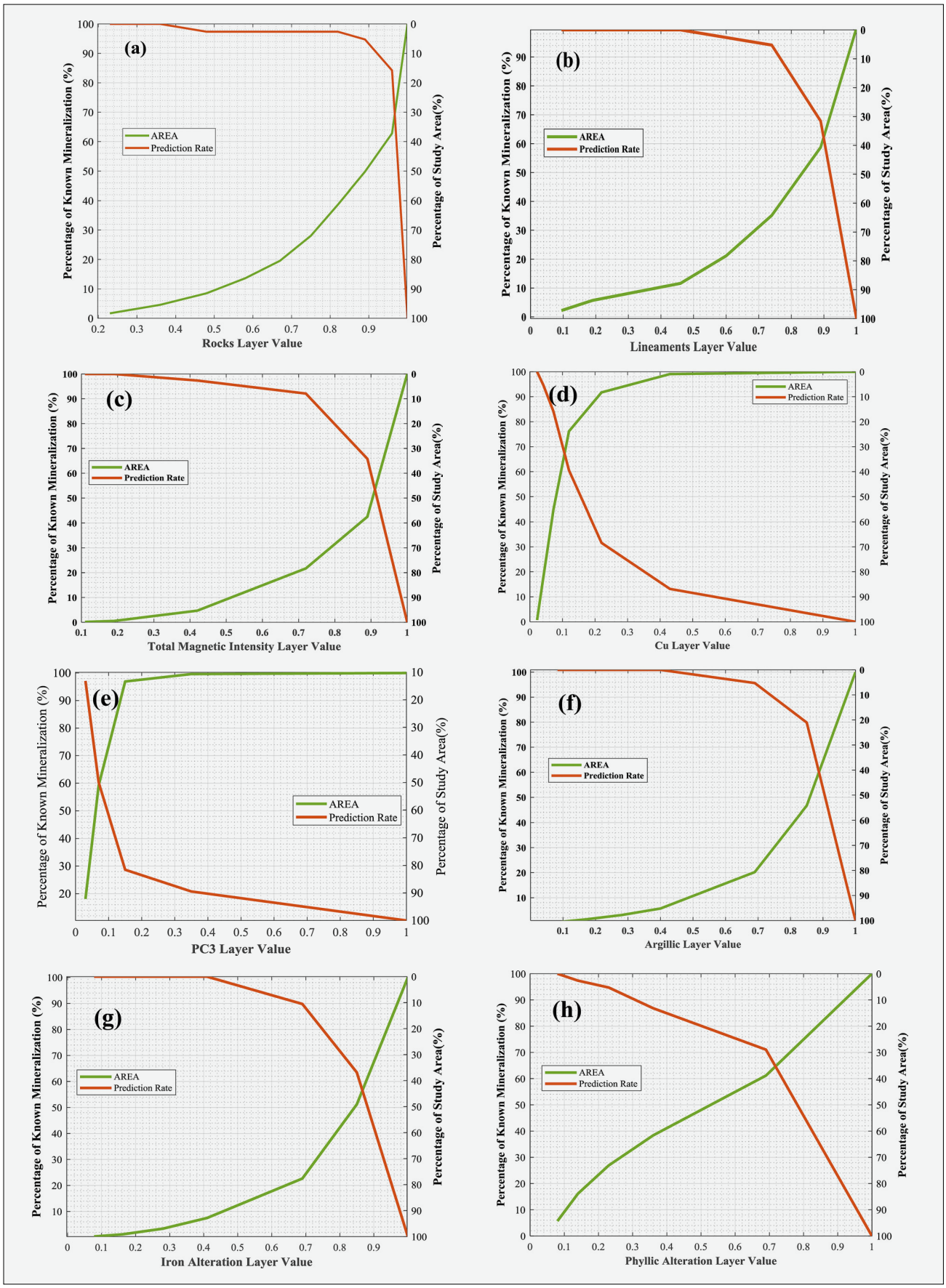

Figure 8. Prediction- area plot (P-A) for (a) subvolcanic units (b) Lineament density (c) aeromagnetic anomalies (d) Cu signature (e) Multivariate geochemistry signature (f) argillic alteration (g) iron oxide alteration (h) phyllic alteration.

Table 6. Calculated weights using P-A plots

Map	Prediction rate (P_r)%	Occupied area (O_a)%	Normalized Density (N_d)	Weight (W_e)
Lithology	70	30	2.33	0.84
Lineaments	63	37	1.7	0.53
Geophysics	56	44	1.27	0.23
Cu Signature	68	32	2.12	0.75
PC3	61	39	1.56	0.44
Argillic alteration	60	40	1.5	0.4
Iron-oxide alteration	59	41	1.43	0.35
Phyllic alteration	67	33	2.03	0.7

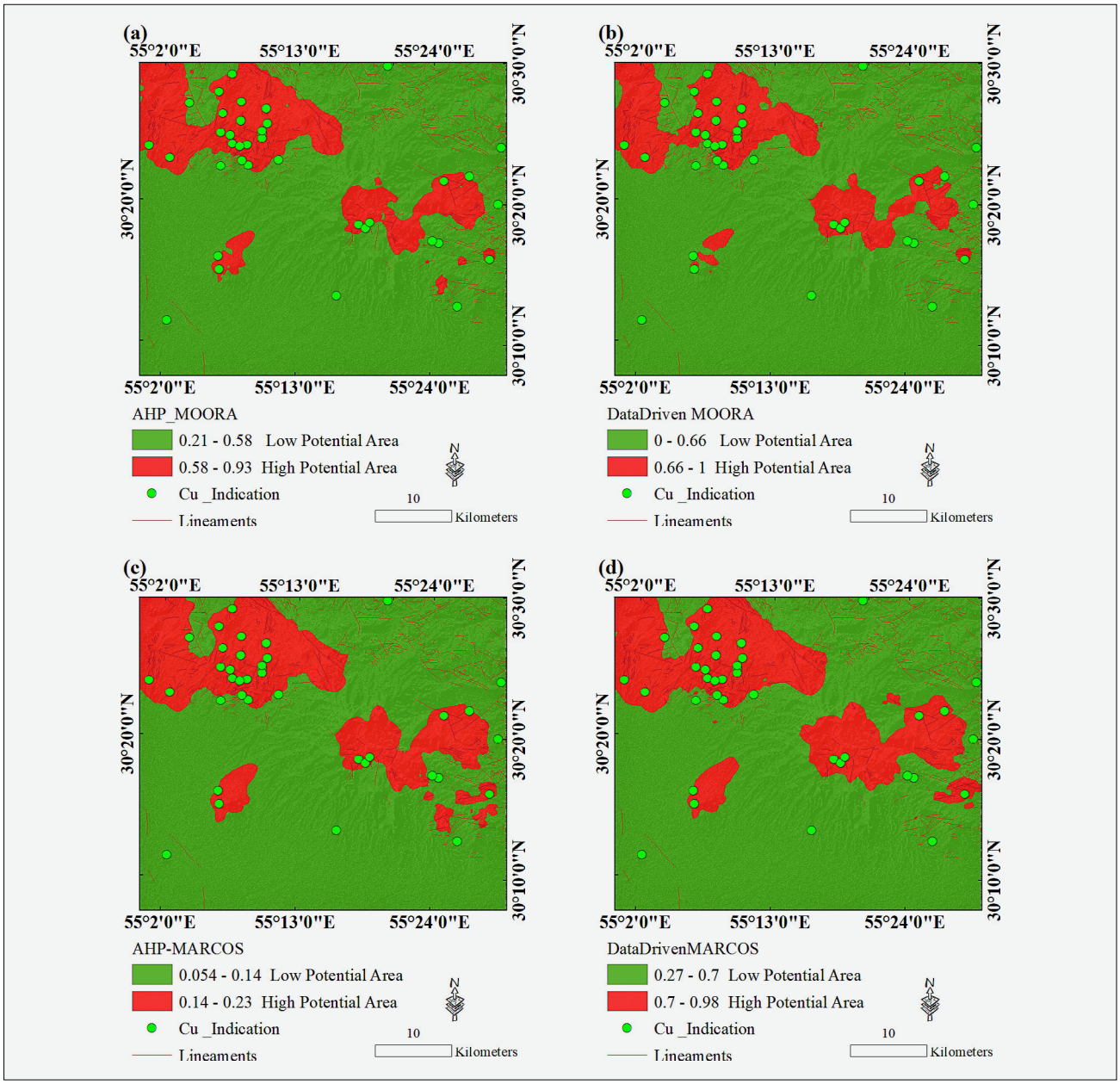

Figure 9. Mineral prospectivity model (a) MARCOS method (b) MOORA method (c) AHP MARCOS (d) Data-Driven MARCOS.

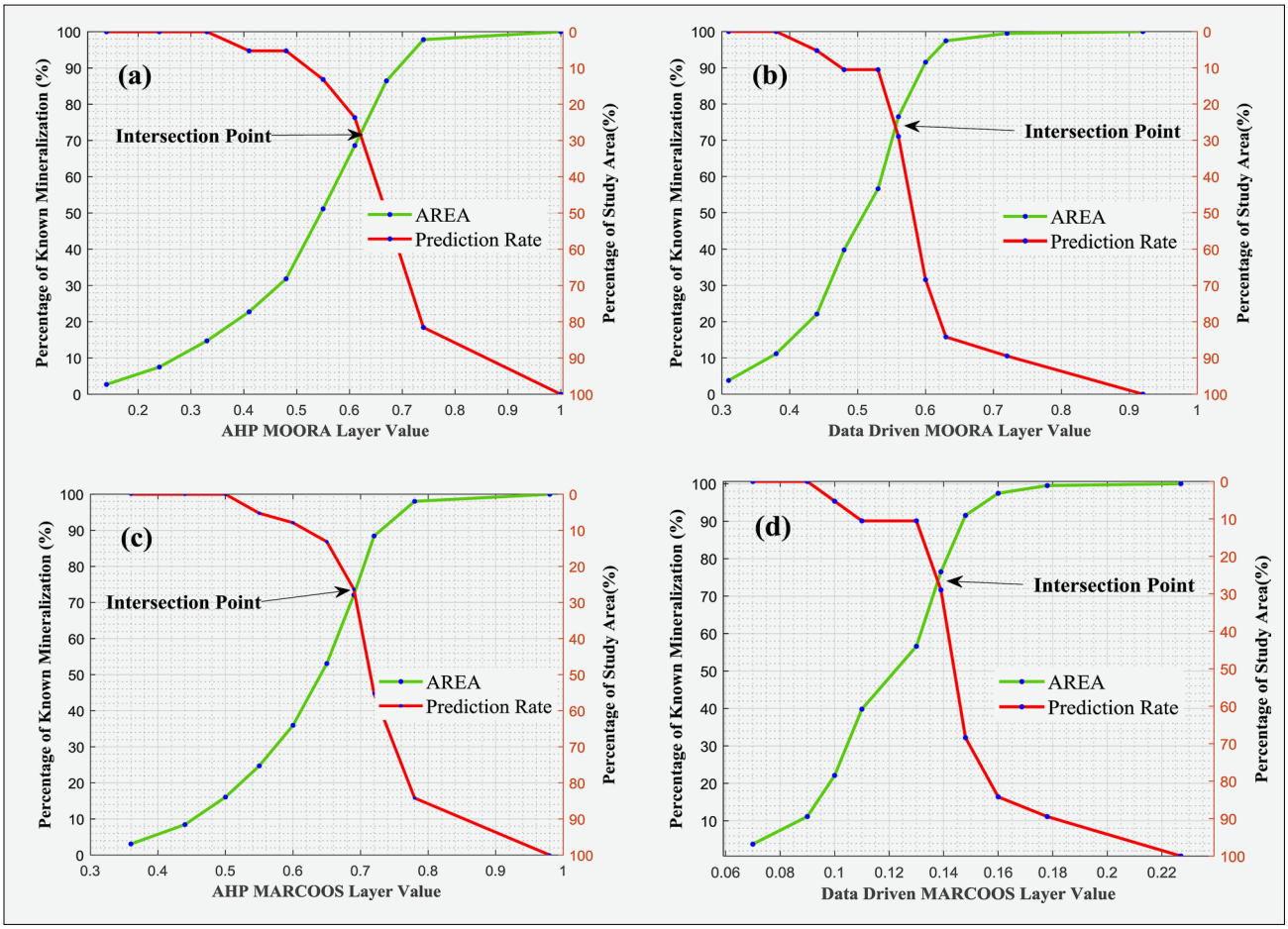

Figure 10. Prediction- area plot (P-A) for evaluating mineral prospectivity models: (a) AHP MOORA (b) Data driven MOORA (c) AHP MARCOS (d) Data driven MARCOS.

Table 7. Calculated weights using P-A plots

Map	Prediction rate (P_r)%	Occupied area (O_a)%	Normalized Density (N_d)	Weight (W_c)
AHP MOORA	72	28	2.57	0.94
Data Driven MOORA	74	26	2.84	1.04
AHP MARCOS	73	27	2.70	0.99
Data Driven MARCOS	75	25	3.00	1.09

tivariate geochemical layers, as well as the subvolcanic intrusive body layer. Visually, acquired models obtained using knowledge-based methods (see **Figure 9**) show a good agreement between the existence of porphyry copper mineralization indices in the area and the areas with high potential (see **Figure 8a** and **c**).

Unlike knowledge-driven methods, data-driven methods apply existing exploratory evidential layers and Cu indices for weighting. The basis of weighting in the data-driven method is the use of P-A plots. The weights obtained from the P-A plot method show that the highest weight is related to the subvolcanic layer. After that, the highest weight is related to the univariate geochemical layer of the copper element. The phyllic alteration, fault layer, multivariate geochemical layer, argillic alteration, iron oxide alteration, and airborne geophysical layer are in the following ranks, respectively (see **Table 3**). The weights obtained from the P-A plot method for the lithology layer, univariate geochemistry, phyllic alteration, fault layer, multivariate geochemistry layer, argillic alteration layer, and airborne geophysics layer are 0.84, 0.75, 0.7, 0.53, 0.44, 0.4, 0.35, and 0.23, respectively (Jenks' discretization method was applied to draw the P-A plot diagram). Then, with the assignment of these weights on the exploratory evidential layers, the MOORA and MARCOS. methods were implemented to generate a mineral potential model (see **Figure 8b** and **d**). By comparing the models obtained from knowledge-based and data-based methods, the highest probability of mineralization potential is in the northwestern part of the study area. Also, a high potential area is observed in the eastern part of the area.

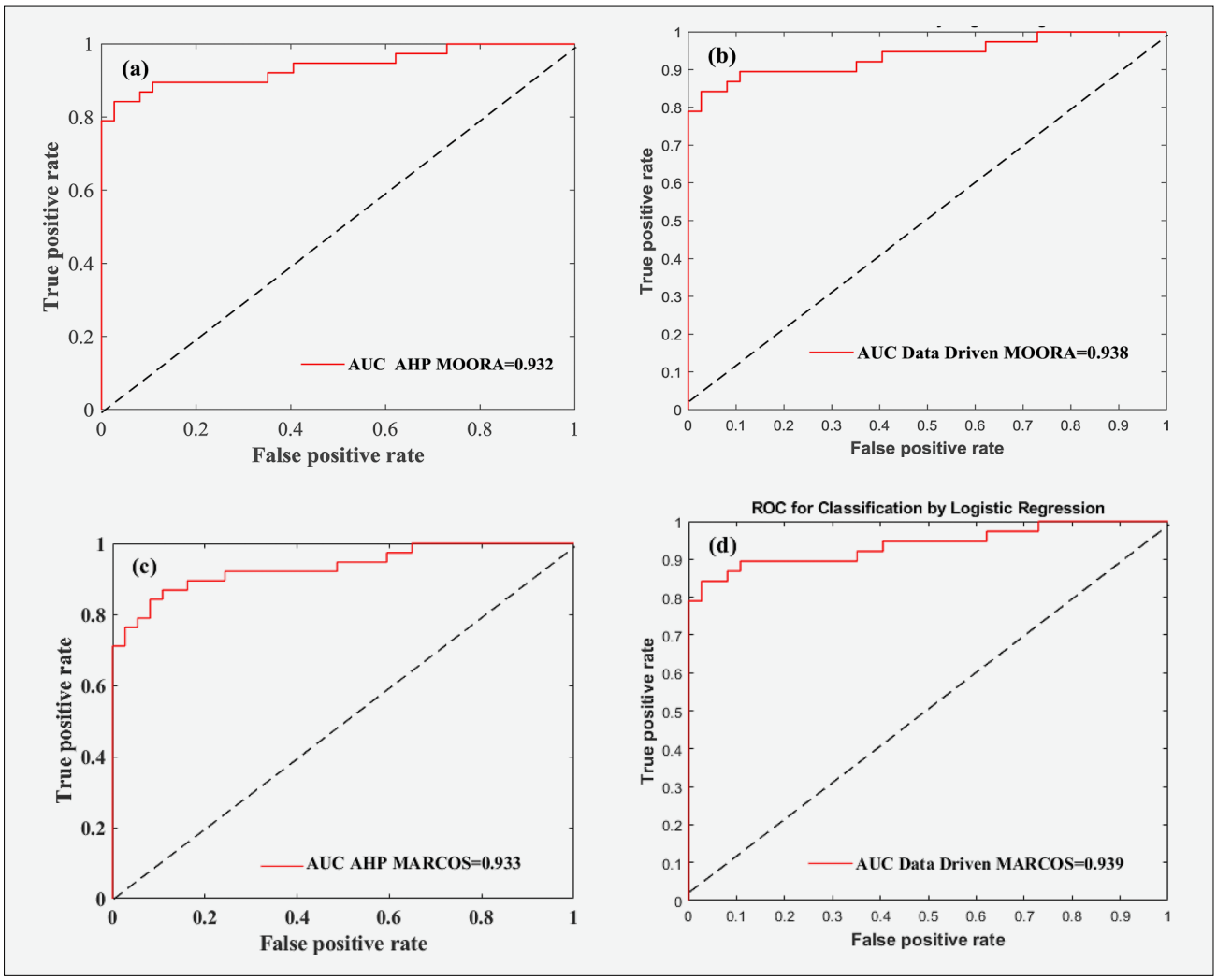

Figure 11. The area under the curve for evaluating mineral prospectivity models
(a) AHP MOORA model (b) Data-driven MOORA (c) AHP MARCOOS (d) Data-Driven MARCOS model.

Unlike knowledge-driven methods, data-driven methods apply existing exploratory evidential layers and Cu indices for weighting. The basis of weighting in the data-driven method is the use of P-A plots. The weights obtained from the P-A plot method show that the highest weight is related to the subvolcanic layer. After that, the highest weight is related to the univariate geochemical layer of the copper element. The phyllic alteration, fault layer, multivariate geochemical layer, argillic alteration, iron oxide alteration, and airborne geophysical layer are in the following ranks, respectively (see **Table 3**). The weights obtained from the P-A plot method for the lithology layer, univariate geochemistry, phyllic alteration, fault layer, multivariate geochemistry layer, argillic alteration layer, and airborne geophysics layer are 0.84, 0.75, 0.7, 0.53, 0.44, 0.4, 0.35, and 0.23, respectively (Jenks' discretization method was applied to draw the P-A plot diagram). Then, with the assignment of these weights on the exploratory evidential layers, the MOORA and MARCOS methods were implemented to generate a mineral potential model (see **Figure 8b** and **d**). By comparing the models obtained from knowledge-based and data-based methods, the highest probability of mineralization potential is in the northwestern part of the study area. Also, a high potential area is observed in the eastern part of the area.

By comparing the models produced using data-driven and knowledge-driven methods, it becomes clear that the models produced by data-driven methods have a stronger correlation with Cu porphyry indices. Also, the data-driven MARCOS method has a greater ability than the other three models in producing a mineral potential model. In the data-driven MARCOS method, 75% of the Cu indices are located in the potential areas while, this value is 74% for the data-driven MOORA method. The prediction rates for the knowledge-driven MOORA and MARCOS methods are 73% and 72%, respectively.

A quantitative comparison between the models generated using the ROC method is performed. Based on the results of this method, it is clear that the performance of the four modelling methods is very similar to each other. However, the model generated by the data-driven MAR-

COS method shows a slightly better performance than the other three methods.

This research, like other research, faces limitations. For example, the preparation of data by the relevant organizations. The reason for this limitation is its high cost. Another limitation is the lack of gold analysis. The presence of gold analysis could lead to better results in generating a mineral potential model.

6. Conclusions

The present study introduces the MARCOS method as a multivariate decision-making approach for producing mineral potential models. Also, in this study, a comparison has been made between models produced using knowledge-based and data-based methods. Another goal of this study is to reduce the uncertainty caused by expert opinions by relying on data-based methods. A quantitative comparison has been made between different models produced using the P-A plot and the ROC methods. Based on this comparison, data-based methods have produced models with higher accuracy, and the MARCOS data-based method has also produced a better model than the other three methods. The prediction rate for the data-driven MARCOS method is 75%, which is the highest prediction rate among the produced models.

7. References

Abedi, M., Norouzi, G.-H., & Bahroudi, A. (2012). Support vector machine for multi-classification of mineral prospectivity areas. Computers & Geosciences, 46, 272–283. https://doi.org/10.1016/j.cageo.2011.12.014

Moon, W. M. (1990). An evidential reasoning structure for integrating geophysical, geological and remote sensing data. Proceedings of IGARSS '93 - IEEE International Geoscience and Remote Sensing Symposium, 1359–1361. https://doi.org/10.1109/IGARSS.1993.322084

Bonham-carter, G. F., & Agterberg, F. P. (1999). Arc-WofE : a GIS tool for statistical integration of mineral exploration datasets. Bulletin of the International Statistical Institute, 52.

Brown, W. M., Gedeon, T. D., Groves, D. I., & Barnes, R. G. (2000). Artificial neural networks: A new method for mineral prospectivity mapping. Australian Journal of Earth Sciences, 47(4), 757–770. https://doi.org/10.1046/j.1440-0952.2000.00807.x

Carranza, E. J. M. (2010). Improved Wildcat Modelling of Mineral Prospectivity. Resource Geology, 60(2), 129–149. https://doi.org/10.1111/j.1751-3928.2010.00121.x

Carranza, E. J. M., & Hale, M. (1997). A catchment basin approach to the analysis of reconnaissance geochemical-geological data from Albay Province, Philippines. Journal of Geochemical Exploration, 60(2), 157–171. https://doi.org/10.1016/S0375-6742(97)00032-0

Feizi, F., Karbalaei-Ramezanali, A. A., & Farhadi, S. (2021). FUCOM-MOORA and FUCOM-MOOSRA: new MCDM-based knowledge-driven procedures for mineral potential mapping in greenfields. SN Applied Sciences, 3(3), 358. https://doi.org/10.1007/s42452-021-04342-9

Jahantigh, M., & Ramazi. H. (2025-a). Knowledge Driven methods for Cu-Au Porphyry Potential Modelling; a case study of the Mokhtaran area, Eastern Iran. Journal of Mining and Environment.

Jahantigh, M., & Ramazi. H. (2025-b). Mineral Prospectivity Modeling with Airborne Geophysics and Geochemistry Data: a Case Study of Shahr-e-Babak Studied Area, Southern Iran. Journal of Mining and Environment.

Jahantigh, M., & Ramazi. H. (2024). Integration of Airborne Geophysics Data with Fuzzy c-means Unsupervised Machine Learning Method to Predict Geological Map, Shahr-e-Babak Study Area, Southern Iran. Journal of Mining and Environments, 273–287.

Karbalaeiramezanali, A., Parsa, M., Lentz, D. R., & Thorne, K. G. (2025). Prospectivity Modeling of Devonian Intrusion-Related W–Mo–Sb–Au Deposits in the Pokiok Plutonic Suite, West-Central New Brunswick, Canada, Using a Monte Carlo-Based Framework. Natural Resources Research, 34(2), 669–702. https://doi.org/10.1007/s11053-024-10437-y

Mami Khalifani, F., Lentz, D., Walker, J., & Khammar, F. (2025). Applying Mineral System Criteria to Develop a Predictive Modelling for Epithermal Gold Mineralization in Northern New Brunswick: Using Knowledge-Driven and Data-Driven Methods. Minerals, 15(4), 345. https://doi.org/10.3390/min15040345

Mars, J. (2006). Radiometer (ASTER) data and logical operator algorithms arc, Iran, using Advanced Spaceborne Thermal Emission and Reflection Regional mapping of phyllic- and argillic-altered rocks in the Zagros magmatic. Geosphere, 2(3), 161. https://doi.org/10.1130/GES00044.1

Mirzaei Misagh, A. P. A. A. K. M. Z. Z. A. (2014). Prospection of Iron and Manganese Using Index Overlay and Fuzzy Logic Methods in Balvard 1:100,000 Sheet, SE Iran. Iranian Journal of Earth Sciences, 6(1), 1–11.

Nykänen, V., Groves, D. I., Ojala, V. J., Eilu, P., & Gardoll, S. J. (2008). Reconnaissance-scale conceptual fuzzy-logic prospectivity modelling for iron oxide copper – gold deposits in the northern Fennoscandian Shield, Finland. Australian Journal of Earth Sciences, 55(1), 25–38. https://doi.org/10.1080/08120090701581372

Parsa, M., Maghsoudi, A., Yousefi, M., & Sadeghi, M. (2016). Recognition of significant multi-element geochemical signatures of porphyry Cu deposits in Noghdouz area, NW Iran. Journal of Geochemical Exploration, 165, 111–124. https://doi.org/10.1016/j.gexplo.2016.03.009

Pazand, K., Hezarkhani, A., & Ataei, M. (2015). Using TOPSIS approaches for predictive porphyry Cu potential mapping: A case study in Ahar-Arasbaran area (NW, Iran). Computers & Geosciences, 49, 62–71. https://doi.org/10.1016/j.cageo.2012.05.024

Porwal, A., Carranza, E. J. M., & Hale, M. (2003). Artificial Neural Networks for Mineral-Potential Mapping: A Case Study from Aravalli Province, Western India. Natural Resources Research, 12(3), 155–171. https://doi.org/10.1023/A:1025171803637

Riahi, S., Bahroudi, A., Abedi, M., Lentz, D. R., & Aslani, S. (2023). Application of data-driven multi-index overlay

and BWM-MOORA MCDM methods in mineral prospectivity mapping of porphyry Cu mineralization. Journal of Applied Geophysics, 213, 105025. https://doi.org/10.1016/j.jappgeo.2023.105025

Richards, J. P., Boyce, A. J., & Pringle, M. S. (2001). Geologic Evolution of the Escondida Area, Northern Chile: A Model for Spatial and Temporal Localization of Porphyry Cu Mineralization. Economic Geology, 96(2), 271–305. https://doi.org/10.2113/gsecongeo.96.2.271

Safari, M., Maghsoudi, A., & Pour, A. B. (2018). Application of Landsat-8 and ASTER satellite remote sensing data for porphyry copper exploration: a case study from Shahr-e-Babak, Kerman, south of Iran. Geocarto International, 33(11), 1186–1201. https://doi.org/10.1080/10106049.2017.1334834

Shahabpour, J. (1999). The role of deep structures in the distribution of some major ore deposits in Iran, ne of the Zagros thrust zone. Journal of Geodynamics, 28(2–3), 237–250. https://doi.org/10.1016/S0264-3707(98)00040-4

Sillitoe, R. H. (1994). Erosion and collapse of volcanoes: Causes of telescoping in intrusion-centered ore deposits. Geology, 22(10), 945. https://doi.org/10.1130/0091-7613(1994)022<0945:EACOVC>2.3.CO;2

Stević, Ž., Pamučar, D., Puška, A., & Chatterjee, P. (2020). Sustainable supplier selection in healthcare industries using a new MCDM method: Measurement of alternatives and ranking according to COmpromise solution (MARCOS). Computers & Industrial Engineering, 140, 106231. https://doi.org/10.1016/j.cie.2019.106231

Taghipour, N., Aftabi, A., & Ramezani, M. R. (2009). Investigation on the Alteration-Mineralization Haloes and Distribution Patterns of Cu, Au, Ag and Mo in the Miduk Porphyry Copper Deposit, Shahr-Babak, Kerman. Scientific Quarterly Journal of Geosciences, 18(72), 45–54. https://doi.org/10.22071/gsj.2010.57137

Tešić, D., Božanić, D., Puška, A., Milić, A., & Marinković, D. (2023). Development of the MCDM fuzzy LMAW-grey MARCOS model for selection of a dump truck. Reports in Mechanical Engineering, 4(1), 1–17. https://doi.org/10.31181/rme20008012023t

Tshanga M, M., Ncube, L., & van Niekerk, E. (2024). Remote sensing insights into subsurface-surface relationships: Land Cover Analysis and Copper Deposits Exploration. Earth Science Informatics, 17(5), 3979–4000. https://doi.org/10.1007/s12145-024-01423-2

Waterman, G. C., & Hamilton, R. L. (1975). The Sar Cheshmeh porphyry copper deposit. Economic Geology, 70(3), 568–576. https://doi.org/10.2113/gsecongeo.70.3.568

Yousefi, M., & Carranza, E. J. M. (2015). Geometric average of spatial evidence data layers: A GIS-based multi-criteria decision-making approach to mineral prospectivity mapping. Computers & Geosciences, 83, 72–79. https://doi.org/10.1016/j.cageo.2015.07.006

Yousefi, M., Carranza, E. J. M., Kreuzer, O. P., Nykänen, V., Hronsky, J. M. A., & Mihalasky, M. J. (2021). Data analysis methods for prospectivity modelling as applied to mineral exploration targeting: State-of-the-art and outlook. Journal of Geochemical Exploration, 229, 106839. https://doi.org/10.1016/j.gexplo.2021.106839

SAŽETAK

Modeliranje potencijala Cu porfirita korištenjem MARCOS metode vođene podatcima i znanjem, studija slučaja, područje Shahr-e-Babak, jugoistočni Iran

Cilj je ove studije usporediti učinkovitost višekriterijskoga odlučivanja (MCDM) vođenoga podatcima i znanjem u izradi modela mineralnoga potencijala u području istraživanja Shahr-e-Babak u jugoistočnome Iranu. Kako bi se postigao taj cilj, obrađeno je i izrađeno osam slojeva, uključujući geološku podlogu, sadržaj bakra, analizu glavnih komponenti, argilične alteracije, hidrotermalne alteracije, alteracije željezovih oksida (Gossan), geofizičke podatke i linearne strukture. Za izradu optimalnoga modela prvo su svi slojevi skalirani i pomaknuti na interval od nule do jedan. Za izradu modela mineralnoga potencijala u istraživanome području uvedena je MARCOS metoda (alternativna mjerenja i rangiranje prema kompromisnome rješenju). Za ponderiranje kontrolnoga sloja korištene su dvije metode: metoda stope predviđanja površine (P-A) i metoda analitičkoga hijerarhijskog procesa (AHP). Zatim su rezultati uspoređeni s metodom višekriterijske optimizacije analizom omjera (MOORA) koja je dokazanu u procjeni mineralnoga potencijala. Za usporedbu ovih metoda korištene su dvije metode – stopa predviđanja površine i površina ispod krivulje (AUC). Rezultati su pokazali da MARCOS pristup vođen podatcima pruža najbolje performanse i prikazuje najbolji model mineralnoga potencijala. Normalizirana gustoća za MARCOS metodu vođenu podatcima, MOORA metodu vođenu podatcima, MARCOS metodu vođenu znanjem te MOORA metodu vođenu znanjem jednaka je 3,00, 2,84, 2,7 i 2,57, dok su AUC vrijednosti iznosile 0,939, 0,938, 0,933 i 0,932.

Ključne riječi:
porfirit, MARCOS, MOORA, područje Shahr-e-Babak, vođeno podatcima

Author's contribution

Moslem Jahantigh (Dr): data curation, formal analysis and software. **Hamidreza Ramazi** (Dr): supervision and validation.
All authors have read and agreed to the published version of the manuscript.